24. THE LATE MIOCENE STABLE ISOTOPE RECORD, SITE 926[1]

N.J. Shackleton[2] and M.A. Hall[2]

ABSTRACT

A continuous $\delta^{18}O$ and $\delta^{13}C$ record in bulk fine-fraction carbonate has been obtained for the late Miocene and late middle Miocene (5–14 Ma) at 10-cm intervals (corresponding to an average 6 k.y.). Continuous data are presented for benthic foraminifers over the interval 5–7.3 Ma as well as over intervals from ~9.5 to 9.8 Ma and 11 to 13 Ma. Limited data are also available for planktonic foraminifers over the same intervals. There is strong orbital-frequency covariance between $\delta^{13}C$ in bulk fine fraction and $\delta^{13}C$ in benthic foraminifers, suggesting that both parameters reflect variability in the $\delta^{13}C$ of dissolved CO_2 in the ocean. Spectral analysis of the whole $\delta^{13}C$ record for bulk fine fraction shows strong power in the 400-k.y. and 100-k.y. eccentricity bands. Benthic $\delta^{18}O$ shows variability that probably reflects the temperature of the deep (3.6 km) Atlantic Ocean water. Bulk fine-fraction $\delta^{18}O$ displays very little high-frequency variability, possibly due to an original signal having been reduced through isotopic equilibration with pore water. The origin of the long-term variability in bulk fine-fraction $\delta^{18}O$, which apparently implies a cooling centered on about 9.5 Ma, is enigmatic, since this feature is not evident in the $\delta^{18}O$ data for *G. sacculifer.*

INTRODUCTION

The sediments recovered during Ocean Drilling Program (ODP) Leg 154 on the Ceara Rise include two complete, well-preserved sections through the upper Miocene, at Sites 925 and 926. This contrasts with the experience of previous drilling in the North Atlantic, including Deep Sea Drilling Project (DSDP) Site 354 that was also drilled on the Ceara Rise (Supko, Perch-Nielsen, et al., 1977), which encountered hiatuses in the upper Miocene. The two Leg 154 sites that were drilled at the greatest water depth penetrated carbonate-free sediment at about 6 Ma (Site 929, 4356 m water depth) and about 7 Ma (Site 928, 4012 m water depth). At Site 926 (3598 m water depth), the entire Miocene section contains carbonate, although samples from the upper Miocene show signs of carbonate dissolution. One of the aims of this investigation was to contribute data that might ultimately lead to a better understanding of the event that caused carbonate dissolution at relatively shallow depths in the western equatorial Atlantic, and which may have been responsible for the frequency of reported hiatuses in this time interval.

The entire upper Miocene section of Site 926 was sampled at 10-cm intervals following the shipboard splice. All samples were washed to provide a record of percent coarse fraction. In these sediments, the coarse fraction is comprised almost entirely of foraminiferal tests, whereas the fine fraction is mainly coccoliths and terrigenous clays. Thus the percentage coarse fraction provides an indication of the extent of dissolution of the foraminifers. Stable isotope data were gathered to learn as much as possible about low- and high-frequency oceanographic variability over this interval of time. Some of these data are discussed more extensively in a companion chapter (Shackleton and Crowhurst, this volume).

METHODS AND RESULTS

All data are assigned ages using the time scale discussed by Shackleton and Crowhurst (this volume). The age model is based entirely on astronomical tuning of the lithological cycles that are clearly present in the sediments, and is therefore independent of the stable isotope data. The tuning was performed using the astronomical data of Laskar et al. (1993) and we have used the same data when performing our time-series analysis.

The samples analyzed were taken in accordance with the shipboard splice so as to obtain a complete coverage of the time interval investigated with minimal overlap between adjacent segments from different holes at the site. We generated four types of data: percent coarse fraction (>63 μm) by weight, stable isotope measurements for bulk fine fraction (<63 μm), benthic foraminifers, and planktonic foraminifers. The percent coarse fraction data are not discussed in this chapter but are used (and illustrated) by Shackleton and Crowhurst (this volume). Benthic foraminifers were picked from the fraction >250 μm (very occasionally supplemented by smaller specimens). The great majority of analyzed picks were either *Cibicidoides wuellerstorfi* or other species of *Cibicidoides* resembling *C. kullenbergi.* However, due to the paucity of specimens, it was not possible to maintain complete homogeneity of types accepted for analysis. Where *Cibicidoides* sp. were not available other genera were selected. The adjustment factors in Table 1 were used to reference analyses to "equilibrium"; these figures have been compiled from various sources. Farrell (1991) provides a critical evaluation for the more important of the species we have used, but the adjustments for some of those that we were obliged to select less frequently are probably no more accurate than ±0.2‰. Table 1 also gives the number of analyses for each species (or mixture of species) and thus gives an indication of the proportion of measurements on less reliable species. Planktonic species *Globigerinoides sacculifer* (to 11.5 Ma) and *G. ruber* (older than 12 Ma) were picked from the 355- to 425-μm size range where available, but in many samples specimens were so scarce (due to dissolution) that it was not possible to select from a narrow size range. Both for picked foraminifers and for fine fraction, hydrogen peroxide was used to remove surface organic contaminants prior to analysis. All isotope measurements were made on gas released in a common acid bath attached either to a VG PRISM mass spectrometer (used chiefly for the smaller samples of benthic foraminifers) or to a VG SIRA mass spectrometer. Analyses are reported referenced to the Vienna Peedee belemnite (VPDB) standard via the marble standard NBS19 (Coplen et al., 1983; Coplen, 1983, pers. comm.). For standard-sized samples (over about 0.1 mg weight), analytical precision is about ±0.05‰, but precision is less good and also less easily quantified for the very small samples of benthic specimens. All data are listed in Tables 2–5 (see the CD-ROM, back pocket, this volume).

Table 1. Adjustment factors used to convert measurements made in different benthic foraminiferal species to an assumed equilibrium value, and abbreviations used in Table 4. The number of analyses for each category is also given.

Number analyzed	Abbreviation	Adjustment $\delta^{18}O$	$\delta^{13}C$	Species name
466	PWUELL	0.64	0.0	*Cibicidoides wuellerstorfi*
104	PWUELCIB	0.5	0.0	*C. wuell.* and another sp.
97	GLOBOCAS	–0.1	0.5	*Globocassidulina subglobosa*
66	CIBKULL	0.64	0.0	*C. kullenbergi*
45	CIB	0.5	0.0	*Cibicidoides* sp.
30	ORID	0.0	n.u.	*Oridorsalis* sp.
21	UVIG	0.0	–0.9	*Uvigerina* sp.
5	NUTT	0.35	0.0	*Nuttalides umbonifera*
5	ORTHO	0.0	n.u.	*Orthomorphina* sp.
5	ORIDGLOB	0.0	n.u.	
4	NUTTCIB	0.5	0.0	
4	GYROIDIN	0.0	n.u.	*Gyroidina* sp.
3	PWUELNUT	0.5	0.0	
3	STILOS	–0.15	n.u.	*Stilostomella* sp.
3	PYRGO	0.0	n.u.	*Pyrgo* sp.
2	UVIGLOB	0.0	n.u.	
2	ORIDGYR	0.0	n.u.	
1	NODO	0.0	n.u.	*Nodosaria* sp.
1	UVIGORID	0.0	n.u.	
1	ORIDCIB	0.0	n.u.	

Note: n.u.= not used because $\delta^{13}C$ data for the species are not considered to be reliable.

Table 2. Weight percent of sediment >63 μm in Site 926 samples.

Core, section, interval (cm)			Depth (mbsf)	Depth (mcd)	Age (Ma)	>63 μm (%)
154-926A	16H-2,	144-146	139.95	157.91	5.173	10.9
154-926A	16H-3,	4-6	140.05	158.01	5.178	17.7
154-926A	16H-3,	14-16	140.15	158.11	5.183	17.1
154-926A	16H-3,	24-26	140.25	158.21	5.188	17.1
154-926A	16H-3,	34-36	140.35	158.31	5.193	15.3
154-926A	16H-3,	44-46	140.45	158.41	5.198	18.5
154-926A	16H-3,	54-56	140.55	158.51	5.203	19.9
154-926A	16H-3,	64-66	140.65	158.61	5.209	18.1
154-926A	16H-3,	74-76	140.75	158.71	5.214	18.1
154-926A	16H-3,	84-86	140.85	158.81	5.219	15.1

Only part of this table is produced here. The entire table appears on the CD-ROM.

The data for benthonic foraminifers (Table 4) are provided both as measured, and after making species-dependent adjustments. Only species-adjusted data are shown on the figures. Table 6 lists the age control points (from Shackleton and Crowhurst, this volume) that were used to assign ages to the samples.

Carbon isotope data for bulk fine fraction and for benthic foraminifers are shown in Figure 1. The data for fine fraction show a distinct long-term trend from values around +2‰ between 13 and 14 Ma to values around +1‰ at 5 Ma. A rather sharp drop is apparent at about 11 Ma; values between about 9 and 11 Ma are similar to values between 5 and 6 Ma, with a broad low-amplitude maximum centered at about 8 Ma. These features are also present in the records from the eastern equatorial Pacific that were reported by Shackleton and Hall (1995). There is a considerable amount of higher frequency variability present with an amplitude of almost 1‰; it is difficult to compare this variability with that present in the Pacific because the bulk samples that were analyzed by Shackleton and Hall (1995) had been homogenized in 1.5-m sections. The trend in the $\delta^{13}C$ data is also consistent with that observed by Mead et al. (1991) in fine fraction from ODP Site 704 over the interval from 5 to 8 Ma where our data overlap theirs.

Figure 2 shows the data for the interval 5–7 Ma on an expanded scale. It is apparent on Figure 2 that although there are significant differences between the fine fraction and the benthic foraminiferal records, they share many features that probably represent global ocean $\delta^{13}C$ variability.

Figure 3 shows the available $\delta^{18}O$ data vs. age. At least on the basis of the limited sampling available, the long-term trend towards more positive $\delta^{18}O$ values in benthic foraminifers has a very small amplitude (less than 0.5‰) over the interval 14–5 Ma. Significantly isotopically lighter values are reported by Flower et al. (Chapter 30, this volume) in benthic foraminifers from slightly older material. A similarly slight trend is apparent in our $\delta^{18}O$ data for bulk fine fraction and for planktonic foraminifers. Superimposed on the long-term trend, the bulk fine fraction displays an interval of more positive $\delta^{18}O$ values centered around 9.5 Ma. The more limited data for benthic and for planktonic foraminifers suggest that this feature may only be present in the record for bulk fine fraction.

Figure 4 shows the $\delta^{18}O$ data for benthic foraminifers over the interval 5–7 Ma on an expanded scale. It is evident that the data are quite noisy. This is probably due partly to the small weight of carbonate represented in many of the samples, and partly to the inherent noisiness in measurements utilizing only one or two individuals. In view of the noisiness (which we propose to reduce by making duplicate analyses), we have not attempted to compare our data with those obtained by Hodell et al. (1994) from the Salé Briqueterie section in Morocco. However, in another paper (Shackleton and Crowhurst, this volume) we show that the benthic $\delta^{18}O$ data do exhibit variance that is coherent with orbital obliquity variability, as was reported by Hodell et al. (1994) for the Moroccan data set.

CARBON ISOTOPES

Figure 1 shows $\delta^{13}C$ data for bulk fine fraction and for benthic foraminifers. The measurements for benthic foraminifers other than *Cibicidoides* sp. are referenced to *Cibicidoides* using the adjustment factors given in Table 1. Data for $\delta^{13}C$ in *Oridorsalis* sp. and several other genera are not used here because (at least when selected at the generic level) these groups do not appear to yield consistent $\delta^{13}C$ data. To the first order, the two records are quite similar between 5 and 7 Ma, suggesting that the signal of varying ocean $\delta^{13}C$ dominates both records. Cross-spectral analysis over the interval 5–7 Ma (Figure 5) also shows high coherence between the two $\delta^{13}C$ records. The two records also share high-frequency variability in the 11–13 Ma interval, but the mean difference between the $\delta^{13}C$ values for bulk fine fraction and for benthic foraminifers is significantly greater in this interval compared with the more recent one; the fine fraction is relatively more enriched in ^{13}C (and shows more low-frequency variability) between 11 and 13 Ma than between 5 and 7 Ma. It is possible that this indicates a period of reduced productivity, but more work would be needed to support this speculation. The long-term trend in the $\delta^{13}C$ of bulk sediment or of bulk fine fraction has been interpreted in terms of a decrease since the middle Miocene in the global inventory of organic carbon (Shackleton, 1987). However, the fact that the long-term trend is not the same in the fine fraction as in foraminifers is curious and supports the notion that we do not adequately understand the global significance of the marine $\delta^{13}C$ record through the Miocene (Broecker and Woodruff, 1992; Shackleton and Hall, 1995).

Figure 6 shows a cross-spectral analysis of the whole fine-fraction $\delta^{13}C$ record against an orbital "etp" signal (this "etp" sequence combines eccentricity with an arbitrary amplitude, obliquity, and precession in the relative proportions observed in summer insolation at 65°N [Laskar et al., 1993]). There is significant coherent power at the obliquity frequency and also in the eccentricity band, but essentially none in the precession band. In many circumstances, it would be difficult to detect a precession-related signal with a 6-k.y. sampling interval, but here our time scale is based on sampling at a closer interval and both percent coarse fraction and benthic $\delta^{18}O$ have coherent power in the precession band when sampled at 6-k.y. intervals (Shackleton and Crowhurst, this volume), so that the lack of a precession-related signal in the $\delta^{13}C$ record from bulk fine fraction is not a sampling artifact. Moreover, there is a significant phase difference in the

Table 3. δ¹⁸O and δ¹³C data for bulk fine fraction (<63 µm) in Site 926, referred to the VPDB standard.

Core, section, interval (cm)			Depth (mbsf)	Depth (mcd)	Age (Ma)	Lab code	18O VPDB (per mil)	13C VPDB (per mil)	Fraction	Treat-ment
154-926A	16H-2,	144-146	139.95	157.91	5.173	S 95/1671	0.06	1.18	FINE	P
154-926A	16H-3,	4-6	140.05	158.01	5.178	S 95/1672	0	1.19	FINE	P
154-926A	16H-3,	14-16	140.15	158.11	5.183	S 95/1673	0.07	1.09	FINE	P
154-926A	16H-3,	24-26	140.25	158.21	5.188	S 95/1674	0.17	1.2	FINE	P
154-926A	16H-3,	34-36	140.35	158.31	5.193	S 95/1675	0.07	1.29	FINE	P
154-926A	16H-3,	44-46	140.45	158.41	5.198	S 95/1676	0.1	1.26	FINE	P
154-926A	16H-3,	54-56	140.55	158.51	5.203	S 95/1677	0.15	1.26	FINE	P
154-926A	16H-3,	64-66	140.65	158.61	5.208	S 95/1678	0.09	1.18	FINE	P
154-926A	16H-3,	74-76	140.75	158.71	5.213	S 95/1679	0.35	1.27	FINE	P
154-926A	16H-3,	84-86	140.85	158.81	5.218	S 95/1680	0.24	1.28	FINE	P

Note: P = peroxide treatment of sample.

Only part of this table is produced here. The entire table appears on the CD-ROM.

Table 4. δ¹⁸O and δ¹³C data for picked benthic foraminifers in Site 926, referred to the VPDB standard, and after adjusting according to Table 1.

Core, section, interval (cm)			Depth (mbsf)	Depth (mcd)	Age (Ma)	Lab code	Taxa	18O VPDB (per mil)	13C VPDB (per mil)	Corrected 18O VPDB (per mil)	Corrected 13C VPDB (per mil)
154-926A	16H-2,	144-146	139.95	157.91	5.173	PZ95/701	CIBKULL	2.45	0.65	3.09	0.65
154-926A	16H-3,	4-6	140.05	158.01	5.178	PZ95/702	PWUELL	1.98	1.14	2.62	1.14
154-926A	16H-3,	14-16	140.15	158.11	5.183	PZ95/704	GLOBOCASS	2.67	0.3	2.57	0.8
154-926A	16H-3,	14-16	140.15	158.11	5.183	PZ95/703	PWUELCIB	1.98	1.06	2.48	1.06
154-926A	16H-3,	24-26	140.25	158.21	5.188	PZ95/705	PWUELCIB	2.09	1.06	2.59	1.06
154-926A	16H-3,	34-36	140.35	158.31	5.193	PZ95/706	PWUELL	1.99	1.22	2.63	1.22
154-926A	16H-3,	44-46	140.45	158.41	5.198	PZ95/707	CIBKULL	2.13	1.05	2.77	1.05
154-926A	16H-3,	54-56	140.55	158.51	5.203	PZ95/708	PWUELCIB	2	0.9	2.5	0.9
154-926A	16H-3,	64-66	140.65	158.61	5.209	PZ95/709	PWUELL	1.85	1.05	2.49	1.05
154-926A	16H-3,	74-76	140.75	158.71	5.214	PZ95/710	GLOBOCASS	2.53	0.34	2.43	0.84

Notes: NA = those genera (Table 1) for which the δ¹³C are not used. For species code abbreviations see Table 1.

Only part of this table is produced here. The entire table appears on the CD-ROM.

Table 5. δ¹⁸O and δ¹³C data for picked planktonic foraminifers in Site 926, referred to the VPDB standard.

Core, section, interval (cm)			Depth (mbsf)	Depth (mcd)	Age (Ma)	Lab code	Species	18O VPDB	13C VPDB
154-926A	16H-2,	144-146	139.94	157.9	5.173	S95/1608	GSACC	-0.97	1.85
154-926A	16H-3,	4-6	140.04	158	5.178	S95/1609	GSACC	-1.28	2.25
154-926A	16H-3,	14-16	140.14	158.1	5.183	S95/1610	GSACC	-1.34	2.38
154-926A	16H-3,	24-26	140.24	158.2	5.188	S95/1611	GSACC	-1.35	2.27
154-926A	16H-3,	34-36	140.34	158.3	5.193	S95/1612	GSACC	-1.3	2.38
154-926A	16H-3,	44-46	140.44	158.4	5.198	S95/1613	GSACC	-1.23	2.22
154-926A	16H-3,	54-56	140.54	158.5	5.203	S95/1614	GSACC	-1.13	2.26
154-926A	16H-3,	64-66	140.64	158.6	5.208	S95/1615	GSACC	-1.18	2.3
154-926A	16H-3,	74-76	140.74	158.7	5.213	S95/1616	GSACC	-1.28	2.41
154-926A	16H-3,	84-86	140.84	158.8	5.218	S95/1617	GSACC	-1	2.1

Notes: GSACC denotes *Globigerinoides sacculifer*; GRUBER denotes *G. ruber*; C = picked from the 355- to 425-µm size fraction, a number following C = the number of specimens that otherwise was more than 12, and about 30 where possible.

Only part of this table is produced here. The entire table appears on the CD-ROM.

obliquity band between obliquity and δ¹³C, with positive δ¹³C lagging high-latitude insolation by about 90° (10 k.y.). Both the phase lag with respect to obliquity and the presence of an eccentricity signal, imply that the δ¹³C variability reflects the response of the ocean's dissolved carbon reservoir (time constant ~300 k.y.), rather than that of the ocean circulation system (time constant ~1 k.y.).

It is particularly important to note that the δ¹³C record displays clearly concentrated variance, coherent with eccentricity, both in the 100-k.y. band and at 400 k.y. Moreover the "100-k.y." peak is very clearly split with discrete peaks at 125 k.y. and at 96 k.y., as would be expected if the "100-k.y." peak is associated with orbital eccentricity.

Before considering the origin of the δ¹³C signal associated with orbital eccentricity, it is important to note that (as one would expect) there is considerable aperiodic low-frequency variability in the record and that although the eccentricity peaks are robust and significantly coherent, the coherence is not particularly high so that the coupling between orbital eccentricity and δ¹³C during the Miocene was not strong.

The eccentricity power in the δ¹³C record could have arisen, for example, from climatically controlled changes in organic storage in a marginal sea, in terrestrial biomass, or in the sediments under an upwelling system. We have not explicitly modeled such processes but note that Vincent and Berger (1985) have suggested that the anomalously positive δ¹³C values that are observed in middle Miocene sediments could have arisen from episodes of rapid accumulation of organic carbon due to intense upwelling along the California margin. We suggest that this or analogous processes could have been controlled by orbital time scale climatic variability and that the long res-

Table 6. Age models used to assign ages to the samples analyzed.

Hole	Depth (mcd)	Age (Ma)
926A	121.75	3.903
926A	125.20	4.000
926A	125.90	4.020
926A	127.80	4.076
926A	128.50	4.116
926A	129.20	4.137
926A	129.90	4.160
926A	130.80	4.188
926A	132.30	4.209
926A	133.05	4.231

Notes: Slightly different controls are used in each hole. Age models from Shackleton and Crowhurst, this volume.

Only part of this table is produced here. The entire table appears on the CD-ROM.

idence time of carbon in the ocean could have given rise to the long-period response. The lack of power in the precession band in the $\delta^{13}C$ record strongly indicates that the eccentricity signal is not imparted to the ocean locally in the surface waters of the western tropical Atlantic, but it is conceivable that the origin of the variability could be determined by locating a region where the $\delta^{13}C$ record of surface water does contain power in the precession band. A significant constraint on any explanation of the data is that cross-spectral analysis (Figure 6) shows that ocean $\delta^{13}C$ maxima (i.e. times of maximal organic carbon burial) are associated with eccentricity minima without consistent phase lag. The absence of a lag poses difficulties in invoking the long residence-time of carbon in the ocean as a means of rectifying a forcing on the carbon system arising from precession, just as the small lag between eccentricity and Pleistocene ice volume poses difficulties for attempts to explain the 100-k.y. ice age cycle in terms of eccentricity (Imbrie et al., 1984, Fig. 11).

Woodruff and Savin (1991) provided tantalizing evidence for the possible presence of a 400-k.y. eccentricity signal in the $\delta^{13}C$ record of the middle Miocene on the basis of their estimates of the approximate ages of successive $\delta^{13}C$ maxima. Our demonstration of a clear association between $\delta^{13}C$ and orbital eccentricity in the late Miocene

Figure 1. $\delta^{13}C$ in bulk fine fraction (top; left scale) and in benthic foraminifers (bottom; right scale) from Site 926 vs. age, 5–14 Ma (ages from Shackleton and Crowhurst, this volume).
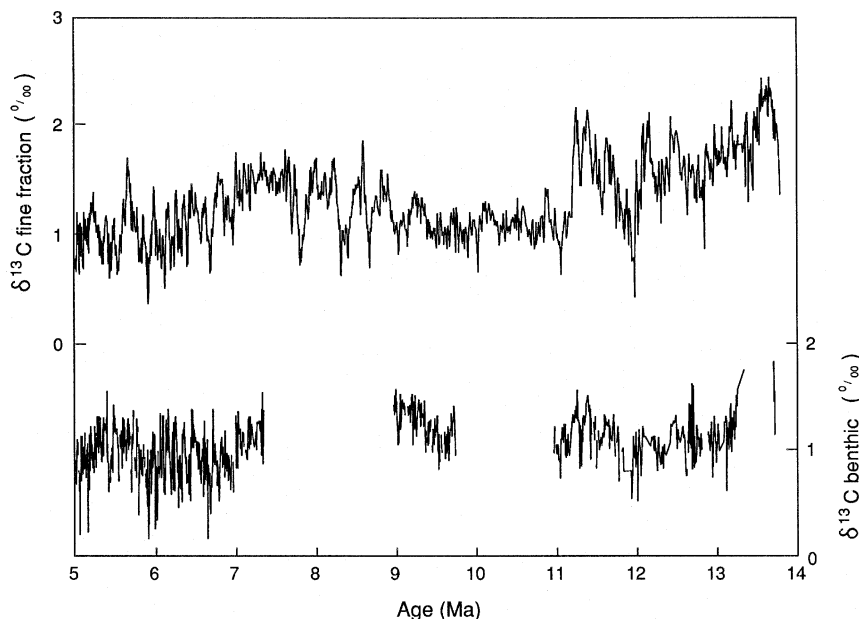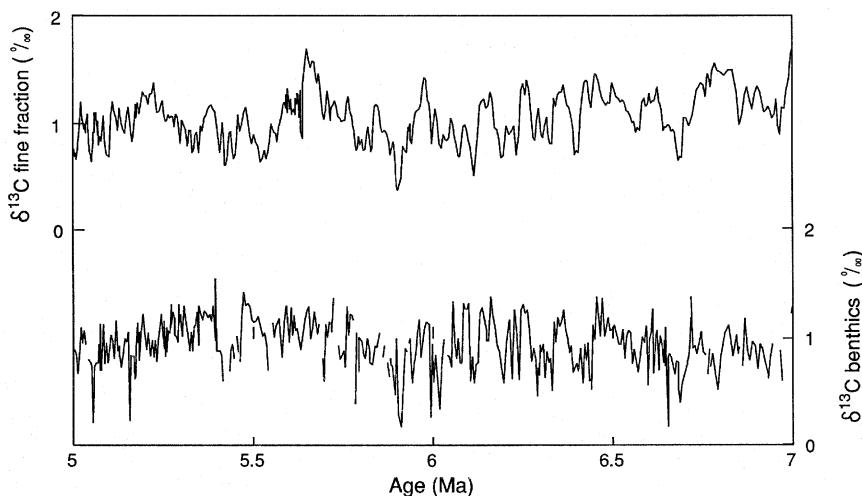

Figure 2. $\delta^{13}C$ in bulk fine fraction (top; left scale) and in benthic foraminifers (bottom; right scale) from Site 926 vs. age, as Fig. 1 but for the interval 5–7 Ma.
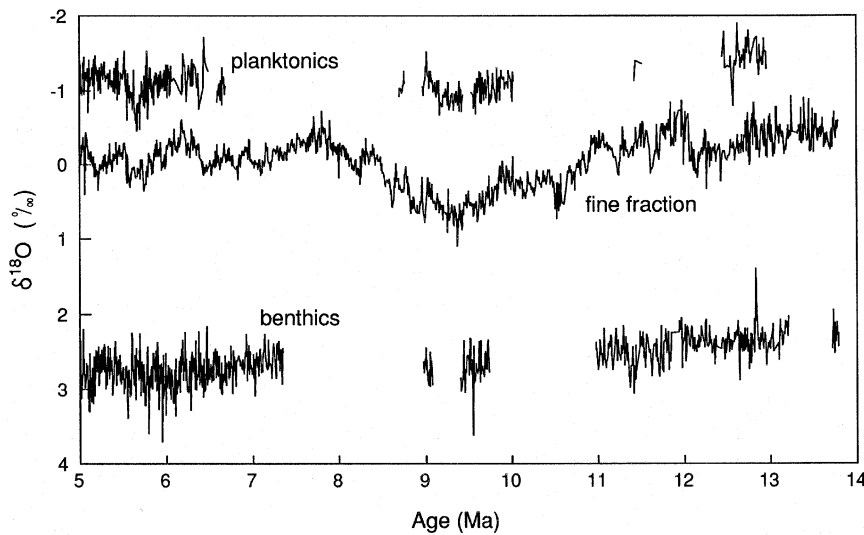
Figure 3. $\delta^{18}O$ in planktonic foraminifers (top, discontinuous); bulk fine fraction (middle, continuous data) and in benthic foraminifers (bottom, discontinuous, species-adjusted according to Table 1), 5–14 Ma.
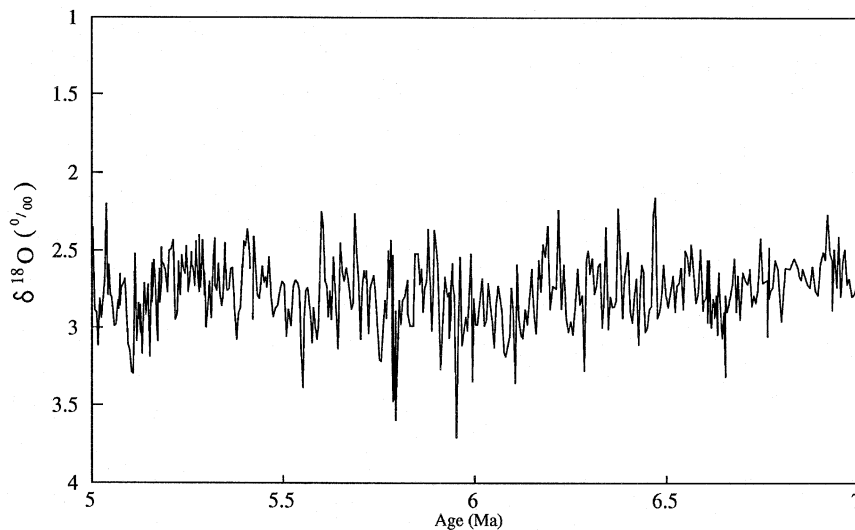

Figure 4. $\delta^{18}O$ in benthic foraminifers (species-adjusted according to Table 1) from Site 926 for the interval 5–7 Ma.

suggests that Woodruff and Savin (1991) were correct in associating their middle Miocene $\delta^{13}C$ cycles with the long eccentricity cycle. This in turn implies that it may be possible to utilize the association between $\delta^{13}C$ and orbital eccentricity as a first stage in astronomical tuning of older segments of the geological record.

OXYGEN ISOTOPES

The oxygen isotope records for bulk fine fraction and for benthic foraminifers (Fig. 3) have little in common at either low or high frequency. So far as the low-frequency variation is concerned, the benthic record is relatively featureless, while the fine-fraction record displays an interval with more positive $\delta^{18}O$ values centered near 9.5 Ma and lasting about 2 million years. Interpreted in terms of temperature, these data would imply a cooling of the surface waters by around 3°C. However, some workers have suggested that changes in the species make-up of the nannofossil fraction could have a significant impact on the $\delta^{18}O$ composition of a mixed nannofossil assemblage (Dudley and Savin, 1979; Lynn and Peterson, 1995). In addition, there may be a significant and varying contribution to the fine fraction from foraminiferal fragments. Measurements were made in benthic foraminifers across a part of this "cool" interval, and there is no cooling evident of the scale implied by the data for bulk fine fraction. Finally, some measurements were made in *G. sacculifer* covering the same interval; although the $\delta^{18}O$ are slightly heavier than the mean for the interval 5–7 Ma, the difference is much smaller than the difference observed in the record for bulk fine fraction. Thus the fine fraction $\delta^{18}O$ data should be used with caution, despite the success achieved by Shackleton and Hall (1995) in interpreting analogous data from East Pacific sediments.

Miller et al. (1991) proposed that the $\delta^{18}O$ record that they derived from the analysis of benthic foraminifers at DSDP Site 608 should be used as a reference section for the Miocene. The record presented here for benthic foraminifers is not sufficiently complete for this concept to be properly evaluated. However, it is possible to make three comments on the basis of a comparison of the data available. First, on the basis of the variability that we observe, it is unlikely that oxygen isotope data from upper Miocene sediments will be of much value as a correlation tool. To further explore their correlation potential, it would be necessary to sample at least as closely as we have done in this study and to improve the precision (by using a larger number of specimens for each analysis). Second, it is possible that the brief deep-water cooling event at about 11.4 Ma (Fig. 3) represents event Mi5 of Miller et al. (1991). Third, the oldest short section that we analyzed for benthic foraminifers is just within the range of *Spheno-*
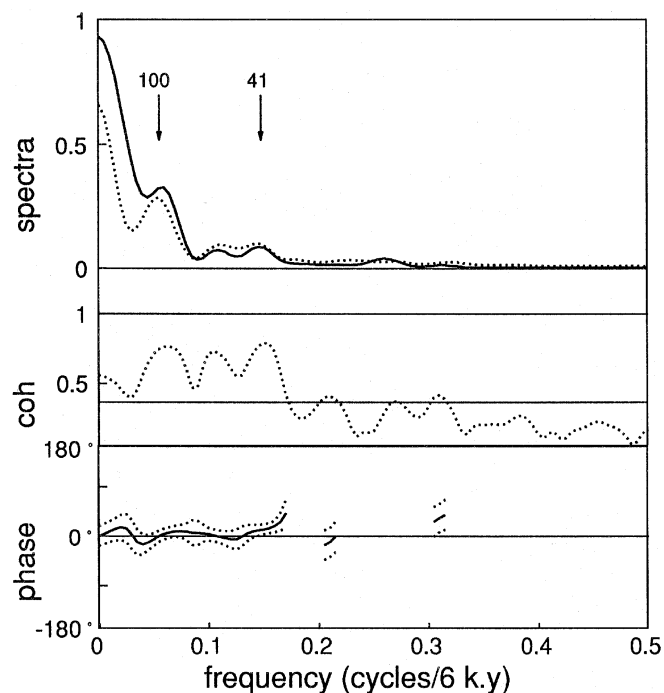
Figure 5. Cross-spectral analysis of δ^{13}C in bulk fine fraction (solid) vs. δ^{13}C in benthic foraminifers (dots), 5–7 Ma. The time series was interpolated at 6-k.y. intervals. At the frequency associated with obliquity (41-k.y. period) and at lower frequencies, the records are coherent (dashed line; middle panel) and in phase (bottom panel).

lithus heteromorphus (Shipboard Scientific Party, 1995) and thus should be correlated with Event Mi3 of Miller et al. (1991) on the basis of the detailed nannofossil data for Site 608 of Olafsson (1991). If so, the data of Miller et al. (1991) give an oversimplified impression of the relationship between benthic δ^{18}O in Mi3 and values later in the Miocene. This conclusion is supported by an examination of the data for DSDP Site 574 (Pisias et al., 1985), where the benthic δ^{18}O values between about 150 and 155 mbsf are isotopically heavy and closer to values later in the Miocene than to values earlier in the middle Miocene. This interval is reported by Pisias et al. (1985) as foraminiferal Zone N10 and according to Olafsson (1989) is within the range of *Sphenolithus heteromorphus*. Therefore, this interval should also be correlative with Event Mi3 of Miller et al. (1991).

SUMMARY

A continuous high-resolution (6 k.y.) stable isotope (δ^{13}C and δ^{18}O) record for bulk fine fraction in Site 926 from about 5 to 14 Ma has been generated. Sections of high-resolution data derived from benthic foraminifers for the intervals between 5 and 7 Ma and 11 and 13 Ma, as well as some data obtained from planktonic foraminifers, put constraints on the interpretation of the data from the fine fraction. There is considerable orbital-frequency variability in ocean δ^{13}C and in benthic δ^{18}O; this means that low-resolution records are liable to alias this variability and will therefore not provide useful data for low-resolution correlation. Using a time scale that is independent of the isotopic data, spectral analysis of the δ^{13}C data shows clearly defined variance associated with the 400-k.y., 125-k.y. and 95-k.y. periodicities of orbital eccentricity as well as the anticipated 41-k.y. periodicity of obliquity of the Earth's rotational axis.

REFERENCES

Broecker, W.S., and Woodruff, F., 1992. Discrepancies in the oceanic carbon isotope record for the last fifteen million years? *Geochim. Cosmochim. Acta,* 56:3259–3264.

Coplen, T.B., Kendall, C., and Hopple, J., 1983. Comparison of stable isotope reference samples. *Nature,* 302:236–238.

Dudley, W.C., and Savin, S.M., 1979. Oxygen isotopic content of coccoliths grown in culture. *Deep Sea Res. Part A,* 26:495–503.

Farrell, J.W., III, 1991. Late Neogene palaeoceanography of the central equatorial Pacific: evidence from carbonate preservation and stable isotopes [Ph.D. dissert.]. Brown Univ., Providence, RI.

Hodell, D.A., Benson, R.H., Kent, D.V., Boersma, A., and Rakic-El Bied, K., 1994. Magnetostratigraphic, biostratigraphic, and stable isotope stratigraphy of an Upper Miocene drill core from the Salé Briqueterie (northwestern Morocco): a high-resolution chronology for the Messinian stage. *Paleoceanography,* 9:835–855.

Imbrie, J., Hays, J.D., Martinson, D.G., McIntyre, A., Mix, A.C., Morley, J.J., Pisias, N.G., Prell, W.L., and Shackleton, N.J., 1984. The orbital theory of Pleistocene climate: support from a revised chronology of the marine δ^{18}O record. *In* Berger, A., Imbrie, J., Hays, J., Kukla, G., and Saltzman, B. (Eds.), *Milankovitch and Climate* (Pt. 1), NATO ASI Ser. C, Math Phys. Sci., 126: Dordrecht (D. Reidel), 269–305.

Laskar, J., Joutel, F., and Boudin, F., 1993. Orbital, precessional, and insolation quantities for the Earth from −20Myr to +10Myr. *Astron. Astrophys.,* 270:522–533.

Lynn, M.J., and Peterson, L.C., 1995. Coccoliths as paleoceanographic indicators of tropical upwelling: late Quaternary records from the Cariaco Basin and Arabian Sea. *ICP V Progr. Abstr.,* 197.

Mead, G.A., Hodell, D.A., Müller, D.W., and Ciesielski, P.F., 1991. Fine-fraction carbonate oxygen and carbon isotope results from Site 704: implications for movement of the Polar Front during the late Pliocene. *In* Ciesielski, P.F., Kristoffersen, Y., et al., *Proc. ODP, Sci. Results,* 114: College Station, TX (Ocean Drilling Program), 437–458.

Miller, K.G., Feigenson, M.D., Wright, J.D., and Clement, B.M., 1991. Miocene isotope reference section, Deep Sea Drilling Project Site 608: an evaluation of isotope and biostratigraphic resolution. *Paleoceanography,* 6:33–52.

Olafsson, G., 1989. Quantitative calcareous nannofossil biostratigraphy of upper Oligocene to middle Miocene sediment from ODP Hole 667A and middle Miocene sediment from DSDP Site 574. *In* Ruddiman, W., Sarnthein, M., et al., *Proc. ODP, Sci. Results,* 108: College Station, TX (Ocean Drilling Program), 9–22.

————, 1991. Quantitative calcareous nannofossil biostratigraphy and biochronology of early through late Miocene sediments from DSDP Hole 608. *Medd. Stockholm Univ. Inst. Geol. Geochem.,* 203.

Pisias, N.G., Shackleton, N.J., and Hall, M.A., 1985. Stable isotope and calcium carbonate records from hydraulic piston cored Hole 574A: high-resolution records from the middle Miocene. *In* Mayer, L., Theyer, F., Thomas, E., et al., *Init. Repts. DSDP,* 85: Washington (U.S. Govt. Printing Office), 735–748.

Shackleton, N.J., 1987. The carbon isotope record of the Cenozoic: history of organic carbon burial and of oxygen in the ocean and atmosphere. *In* Brooks, J., and Fleet, A.J. (Eds.), *Marine Petroleum Source Rocks.* Geol. Soc. Spec. Publ. London, 26:423–434.

Shackleton, N.J., and Hall, M.A., 1995. Stable isotope records in bulk sediment (Leg 138). *In* Pisias, N.G., Mayer, L.A. Janecek, T.R., Palmer-Julson. A. and van Andel, T.H. (Eds.), *Proc. ODP, Sci. Results,* 138: College Station, TX (Ocean Drilling Program) 797−805.

Shipboard Scientific Party, 1995. Site 926. *In* Curry, W.B., Shackleton, N.J., Richter, C., et al., *Proc. ODP, Init. Repts.,* 154: College Station, TX (Ocean Drilling Program), 153−232.

Supko, P.R., Perch-Nielsen, K., et al., 1977. *Init. Repts. DSDP,* 39: Washington (U.S. Govt. Printing Office).

Vincent, E., and Berger, W.H., 1985. Carbon dioxide and polar cooling in the Miocene: the Monterey Hypothesis. *In* Sundquist, E.T., and Broecker, W.S. (Eds.), *The Carbon Cycle and Atmospheric CO₂: Natural Variations Archean to Present.* Geophys. Monogr., Am. Geophys. Union, 32:455−468.

Woodruff, F., and Savin, S.M., 1991. Mid-Miocene isotope stratigraphy in the deep-sea: high resolution correlations, paleoclimatic cycles, and sediment preservation. *Paleoceanography,* 6:755−806.
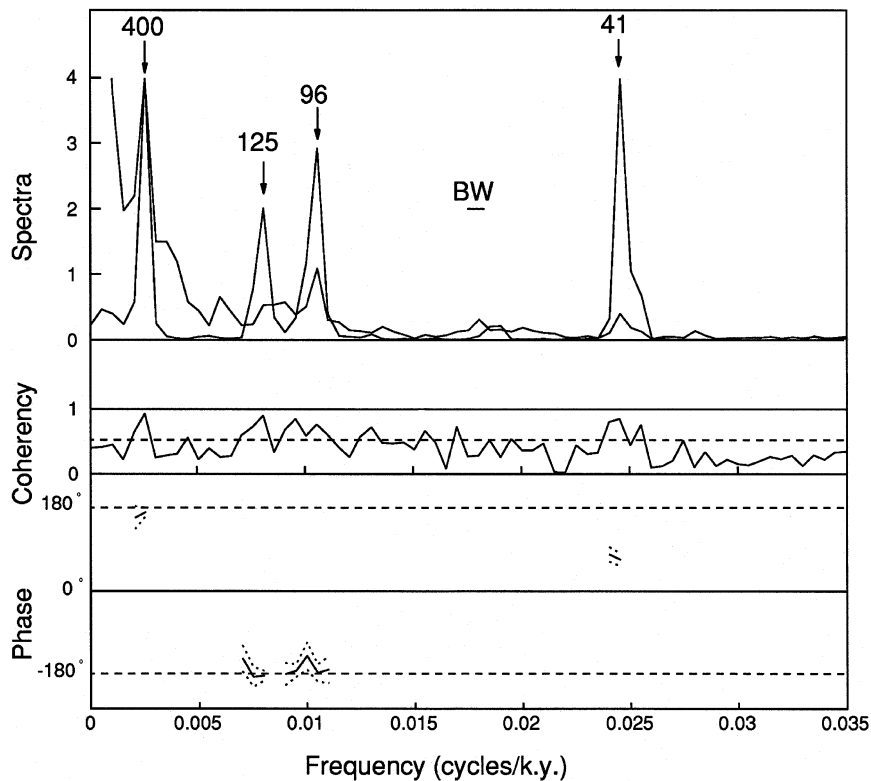
Figure 6. Cross-spectral analysis of $\delta^{13}C$ in bulk fine fraction vs. "etp," 5–14 Ma. There is significant coherency (middle) with eccentricity, especially the 400-k.y. component, as well as with obliquity (but not with precession, which is outside the range displayed here). The phase plot (below) shows that $\delta^{13}C$ is about 180° out of phase with eccentricity, and lags obliquity by almost 90°.